Chromium−Chromium Multiple Bonding in $Cr_2(CO)_9$

Se Li, Nancy A. Richardson, R. Bruce King, and Henry F. Schaefer III*

Department of Chemistry and Center for Computational Quantum Chemistry, University of Georgia, Athens, Georgia 30602

Received: June 30, 2003; In Final Form: September 15, 2003

Density functional theory (DFT) is used to obtain the first structural characterization of the unsaturated dichromium carbonyl $Cr_2(CO)_9$, which is predicted to have a remarkably short metal−metal bond length of 2.31 Å (B3LYP) or 2.28 Å (BP86). This chromium−chromium distance is essentially identical to that reported experimentally for the established Cr≡Cr triple bond in $(\eta^5\text{-}Me_5C_5)_2Cr_2(CO)_4$. The dissociation energy to the fragments $Cr(CO)_4$ and $Cr(CO)_5$ is determined to be 32 kcal/mol (B3LYP) or 43 kcal/mol (BP86). For comparison, the $Cr_2(CO)_{10}$ molecule and the saturated $Cr_2(CO)_{11}$ system have negligible dissociation energies. The minimum energy $Cr_2(CO)_9$ structure is of C_s symmetry with the two chromium atoms asymmetrically bonded to the bridging carbonyls. However, within 0.1 kcal/mol lies a C_2 symmetry structure with one symmetric and two asymmetric bridging carbonyls. Furthermore, the high symmetry D_{3h} structure analogous to $Fe_2(CO)_9$ lies only ∼1 kcal/mol higher in energy. The $Cr_2(CO)_9$ molecule is thus highly fluxional. The extremely flat potential energy surface in the region adjacent to these minima suggests that $Cr_2(CO)_9$ will be labile. The relationship between the $Cr_2(CO)_9$ molecule and the experimentally known binuclear manganese $(\eta^5\text{-}Me_5C_5)_2Mn_2(\mu\text{-}CO)_3$ compound is explored.

1. Introduction

The nature of the metal−metal bond in the absence of the bridging carbonyls (μ_2-CO) in polynuclear metal carbonyls continues to be the subject of considerable discussion. The presence of bridging carbonyls (μ_2-CO) adds to the complexity of the problem owing to alternative possibilities for metal−metal interactions. Although bridging homoleptic unsaturated metal carbonyls have not been isolated in gram quantities under normal laboratory conditions, the synthesis of related organometallic species continues.[1−3] Some very recent work includes the successful synthesis[4] of $(\mu\text{-}S_2)Mn_2(CO)_7$ and the high yield synthesis of the phosphinidene bridged dimolybdenum complex $[Cp_2Mo_2(\mu\text{-}PR)(CO)_4$ (R = 2,4,6-$C_6H_2{}^tBu_3$)].[5] Other and perhaps more important syntheses include the metathesis reactions that involve the M≡M triple bond in bridging $M_2(OH)_6$ and $M_2(SH)_6$ (M = Mo and W) and alkylidene environments which have become crucial in metal mediated preparative procedures.[6] Such experimental work shows the importance of species containing M−M multiple bonds with bridging groups. In addition, new theoretical understandings of these types of multiple bonds may aid in further syntheses and in their use as catalysts.

Metal−metal interactions through metal−carbon bonds to carbonyl groups upon transformation from terminal to semibridging and then to symmetrical bridging carbonyl groups have been studied in the laboratory via the electron density distribution[7] in $[FeCo(CO)_8]^-$. The results showed some evidence for covalent bonds in unsupported metal−metal bonds. However, no bond path was found to directly link the two metals in the bridging carbonyl complex. This result indicated that bridging carbonyls require more metal orbital participation than the terminal carbonyls and thus compete with direct metal−metal interaction.

However, this observation appears to be valid only for iron and cobalt compounds. Thus among the known stable first row transition metal carbonyls, only neutral $Mn_2(CO)_{10}$ (D_{4h} symmetry) lacks bridging carbonyls where only a weak single d−d σ bond exists between the pair of manganese atoms.[8] Iron has one more electron than manganese, so an iron dimer provides two more bonding electrons than the corresponding manganese dimer. In this scheme the additional electrons interact with the bridging carbonyl, and thus no direct metal−metal multiple bond occurs. This accounts for why the singly bonded iron carbonyl $Fe_2(CO)_9$ has been long known while unsaturated bridging homoleptic iron carbonyls with a multiple Fe═Fe or Fe≡Fe bond have not been isolated.[9,10]

In considering the changes from manganese back to chromium in homoleptic binuclear metal carbonyls, we note that the pair of metal atoms provides two fewer electrons for bonding, so that additional ligands are required for each metal atom to achieve the favored 18-electron noble gas configuration. However, the additional ligands are likely to lead to additional repulsion between the coordination spheres of the two metal atoms, thereby hampering the formation of the normal single or double metal−metal bond. This may explain our previous computational results indicating thermodynamic instability for $Cr_2(CO)_{11}$[11] and a long metal−metal distance in singlet $Cr_2(CO)_{10}$.[12] With fewer ligands and d electrons, the possibility of unsaturated compound formation with a multiple metal−metal bond is enhanced greatly.

To this end, we have used theoretical methods to explore the stability of the novel unsaturated species $Cr_2(CO)_9$ with three bridging carbonyls (i.e., $Cr_2(CO)_6(\mu\text{-}CO)_3$). Of particular interest is the existence and nature of the metal−metal multiple bond, together with its most characteristic structural manifestation, namely the metal−metal bond length. Along with optimization of the geometry, we compute the molecular coefficients and the energy levels for all the molecular orbitals (MOs), and analyze which d orbitals give the largest contributions.[13] The symmetry-adapted linear combinations of the d atomic orbitals will provide the bonding and antibonding interactions between

* Corresponding author. E-mail: hfsiii@uga.edu.

10.1021/jp030804b CCC: $25.00
Published on Web 10/29/2003

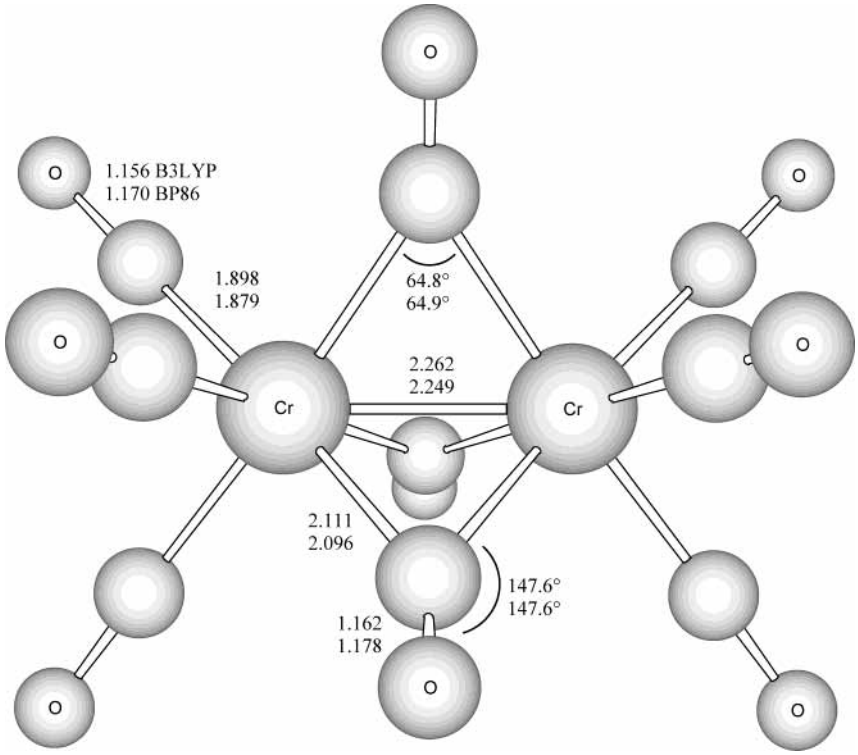

Figure 1. Symmetrically tribridged D_{3h} transition state structure for singlet $Cr_2(CO)_9$. This structure pocesses a significant degenerate imaginary harmonic vibrational frequency for both B3LYP and BP86 functionals. Distances are reported in angstroms.

the metal atoms. The greater the accumulation of electron density, the lower the MO energy, which reflects the metal−metal overlap population values. This elementary concept provides a qualitative description of the d−d binding. Quantitatively this is shown in the electron density plots of the orbitals.

2. Theoretical Methods

Our basis set for C and O begins with Dunning's standard double-ζ contraction[14] of Huzinaga's primitive sets[15] and is designated (9s5p/4s2p). The double-ζ plus polarization (DZP) basis set used here adds one set of pure spherical harmonic d functions with orbital exponents $\alpha_d(C) = 0.75$ and $\alpha_d(O) = 0.85$ to the DZ basis set. For Cr, our loosely contracted DZP basis set, the Wachters' primitive set,[16] is used, but augmented by two sets of p functions and one set of d functions, contracted following Hood, Pitzer, and Schaefer[17] and designated (14s11p6d/10s8p3d). For $Cr_2(CO)_9$, there are 368 contracted Gaussian functions in the present DZP basis set.

Electron correlation effects were included employing density functional theory (DFT) methods, which are acknowledged to be a practical and effective computational tool, especially for organometallic compounds.[18] Among density functional procedures, the most reliable approximation is often thought to be the hybrid Hartree−Fock (HF)/DFT method, B3LYP, which uses the combination of the three-parameter Becke exchange functional with the Lee−Yang−Parr correlation functional.[19,20] However, another DFT method, which combines Becke's 1988 exchange functional with Perdew's 1986 nonlocal correlation functional method (BP86), has proven perhaps even more effective[21] and is also used in this research.[22,23]

We fully optimized the geometries of all structures with the DZP B3LYP and DZP BP86 methods. At the same levels we also computed the vibrational frequencies by analytically evaluating the second derivatives of the energy with respect to the nuclear coordinates. The corresponding infrared intensities are evaluated analytically as well. All of the computations were carried out with the Gaussian 94 program,[24] in which the fine grid (75 302) is the default for evaluating integrals numerically, and the tight (10^{-8} hartree) designation is the default for the self-consistent field (SCF) convergence.

In the search for minima using all currently implemented DFT methods, low-magnitude imaginary vibrational frequencies are suspect because of significant limitations in the numerical integration procedures used in the DFT computations.[9,11,12] Thus, for an imaginary vibrational frequency with a magnitude less than 100 cm^{-1}, there is an energy minimum identical to or very close to the structure of that of the stationary point in question. Therefore, we generally do not follow such low imaginary vibrational frequencies. In the present case the B3LYP and BP86 methods agree with each other fairly well for predicting the structural characteristics of $Cr_2(CO)_9$. The slight discrepancy in the appearance of artifactual imaginary harmonic vibrational frequency remains, however. Population and density analysis procedures use the Gaussian package.

3. Results

3.1. Geometric Conformations. Since $Fe_2(CO)_9$ was found by X-ray crystallography to exhibit a staggered tribridged structure with D_{3h} symmetry,[16] this symmetry was chosen initially for optimization of $Cr_2(CO)_9$ as shown in Figure 1. Viewed from the Cr−Cr axis, each chromium center has a local symmetry of O_h. The computational results show this structure to be a stationary point with a significant degenerate imaginary frequency of 174i (e″) with B3LYP or 138i (e″) with BP86. The three symmetrical bridging CO groups draw the chromium atoms close to each other, leading to a short Cr−Cr distance of 2.262 Å with B3LYP or 2.249 Å with BP86. The terminal carbonyl bond angles are roughly 180°, and the bridging carbonyls are bent to about 147.6°. The Cr−Cr−C angle is 57.5° (B3LYP) or 57.6° (BP86), or alternately, the "bridging angle", the Cr−C−Cr angle, is 64.8° (B3LYP) or 64.9° (BP86). Two

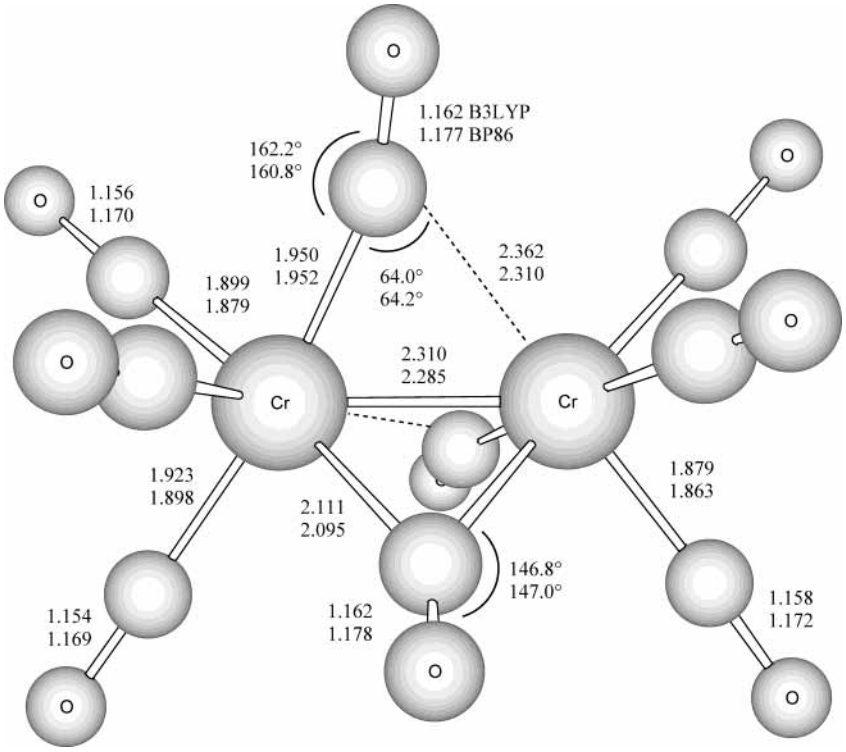

Figure 2. Asymmetrically tribridged BP86 minimum energy structure for singlet $Cr_2(CO)_9$ with C_2 symmetry. This structure has one small imaginary harmonic vibrational frequency for B3LYP and none with the BP86 method. Distances are reported in angstroms.

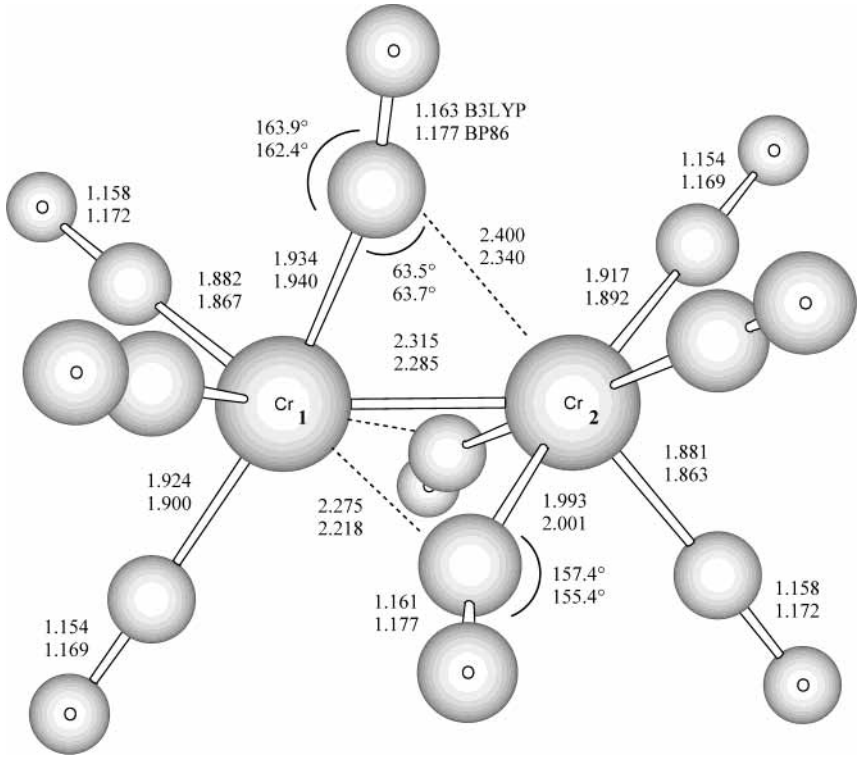

Figure 3. Asymmetrically tribridged B3LYP minimum energy structure for singlet $Cr_2(CO)_9$ with C_s symmetry. This structure has one small imaginary harmonic vibrational frequency for BP86 and none with the B3LYP method. Distances are reported in angstroms.

lower symmetry structures C_2 (Figure 2) and C_s (Figure 3) were obtained by following the degenerate modes of the imaginary frequency.

Notably, the Cr−Cr distances in the $Cr_2(CO)_9$ structures with C_2 and C_s symmetries increase slightly (2.310 and 2.315 Å B3LYP, respectively, and 2.285 BP86 for both). Nevertheless, these Cr−Cr distances are much smaller than those in $Cr_2(CO)_{10}$[21] (2.81 Å B3LYP, 2.68 Å BP86) and $Cr_2(CO)_{11}$[20] (no B3LYP value is available, 3.15 Å BP86). Two (C_s) or three (C_2) bridging CO groups deviate from the central symmetry plane that perpendicularly crosses halfway between the two metal atoms. The structure of C_s symmetry has an asymmetric Cr−Cr bonding mode: one chromium atom is closer to the two bridging carbonyls that reside symmetrically on the opposite sides of the C_s plane. Except for this structural difference for the bridging carbonyls, the predictions are almost exactly the

TABLE 1: Relative Energies of Singlet $Cr_2(CO)_9$ and Its Dissociation Limits $Cr(CO)_4 + Cr(CO)_5$ and $Cr(CO)_3 + Cr(CO)_6$

			imaginary harmonic vibrational frequencies			relative energy (kcal/mol)	
species	sym	state	B3LYP	BP86	HF	B3LYP	BP86
$Cr_2(CO)_9$	D_{3h}	^1A_g	174i (e″)	138i (e″)	203i (e″)	1.7	0.9
	C_2	^1A	55i (b)	none	162i (b)	0.1	0.0
	C_s	$^1A'$	none	22i (a″)	none	0.0	0.0
$Cr(CO)_4 + Cr(CO)_5$	C_{2v} and C_{4v}	$^1A_1$ and $^1A_1$	none	none	none	31.8	42.9
$Cr(CO)_3 + Cr(CO)_6$	C_{3v} and O_h	$^1A_1$ and $^1A_1$	none	none	none	29.8	40.7

TABLE 2: Molecular Orbital Energy Levels and Percentage Contributions of d Atomic Orbitals to the MOs of $Cr_2(CO)_9$ with C_s Symmetry

		largest contributions of the valence atomic orbitals (%)									
MO	energy (eV)										
LUMO+1	−4.52	d_{xy} π*	53,[a] 53[b]								
LUMO	−4.55			d_{yz} π*	54,[a] 53[b]						
HOMO	−6.35	d_{xy} π*	−31, −16					$d_{x^2-y^2}$ σ*	−13, 25	d_{z^2} σ*	58, −47
HOMO−1	−6.40			d_{yz} π*	−23, −26	d_{xz} δ*	64, −47				
HOMO−2	−6.41	d_{xy} π*	−7, −15					$d_{x^2-y^2}$ σ*	−47, 58	d_{z^2} σ*	−37, 7
HOMO−3	−7.08			d_{yz} π	−42, 33	d_{xz} δ	36, 55				
HOMO−4	−7.21	d_{xy} π	−33, 45					$d_{x^2-y^2}$ σ	−33,−5	d_{z^2} σ	27, 47
HOMO−5	−7.43							$d_{x^2-y^2}$ σ	56, 58	d_{z^2} σ	27, 37

[a] The percentage contribution from Cr_1 assigned in Figure 3. [b] The percentage contribution from Cr_2 assigned in Figure 3.

same as for the M−M distance and terminal carbonyls. The bridging angles (Cr−C−Cr) are similar to the above D_{3h} values for C_s 63.6°, 65.3° (B3LYP) or 63.7°, 65.3° (BP86) and, for C_2, 66.4°, 64.0° (B3LYP) or 66.1°, 64.2° (BP86). The similarity of these angles indicates energetic similarity among the structures and supports the idea that the ligands are interacting with the chromium atoms individually rather than through some three-center interaction which would be indicated in the presence of a more obtuse angle. Since the D_{3h} symmetry lies only 2 kcal/mol (B3LYP) or 1 kcal/mol (BP86) higher than C_s and C_2 symmetries which differ only by 0.1 kcal/mol energetically, there are essentially no definite energy preferences for any of the three conformations (energies shown in Table 1). The potential surface in the region adjacent to the three D_{3h}, C_s, and C_2 symmetries is extremely flat, which leads to the effective indistinguishability of the $Cr_2(CO)_9$ structures.

3.2. Vibrational Frequencies. Since the two conformations deviate slightly from D_{3h} symmetry, either of these structures could be considered as minima on the potential energy surface (PES), with the imaginary harmonic vibrational frequency being an artifact of the DFT method. As in previous work,[9,11,12] an interesting contradiction again exists between the B3LYP and BP86 functionals. Only the B3LYP method predicts one imaginary vibrational frequency 55i (b) for the C_2 symmetry structure while, in contrast, only the BP86 method predicts one imaginary frequency 22i (a″) for the C_s symmetry structure.

The B3LYP and BP86 vibrational frequencies for the $Cr_2(CO)_9$ global minimum of C_s symmetry are reported in Table 3. As expected, the CO stretching frequencies have the highest infrared intensities and are expected to dominate the vibrational spectrum. Note also that, for systems such as $Mn_2(CO)_{10}$, $Fe_2(CO)_9$, and $Co_2(CO)_8$, the BP86 method predicts vibrational frequencies more reliably than B3LYP. For $Mn_2(CO)_{10}$, for example, agreement between BP86 and experimental CO stretching frequencies is typically within 10 cm^{-1}.

For the predicted C_s symmetry global minimum (Figure 3), the CO stretches for the semibridging carbonyls are predicted (BP86) at 1919 (a′), 1927 (a″), and 1932 (a′) cm^{-1}. As expected, these three vibrational frequencies lie below the terminal carbonyl stretches, which range from 1970 (a″) to 2060 (a′) cm^{-1}. The most intense infrared fundamental is the terminal a′ CO stretch at 2008 cm^{-1}, with intensity 2213 km/mol.

TABLE 3: Harmonic Vibrational Frequencies (cm^{-1}) and Their Infrared Intensities (km/mol, in Parentheses) for the $Cr_2(CO)_9$ Global Minimum Structure, of C_s Symmetry

B3LYP		BP86	
		a″	
32 (0)	424 (2)	44 (0)	431 (5)
47 (0)	433 (6)	52 (0)	435 (3)
56 (0)	474 (16)	58 (0)	471 (1)
68 (0)	485 (0)	83 (0)	480 (6)
84 (0)	525 (0)	86 (0)	510 (0)
88 (0)	554 (1)	−22 (0)	537 (1)
111 (1)	611 (70)	107 (1)	611 (72)
129 (2)	641 (45)	124 (0)	634 (26)
282 (1)	2016 (673)	274 (0)	1927 (696)
365 (0)	2046 (1306)	374 (0)	1970 (819)
377 (0)	2077 (743)	378 (0)	1987 (721)
414 (12)		422 (0)	
		a′	
45 (2)	450 (5)	48 (2)	464 (10)
77 (0)	464 (39)	73 (0)	474 (7)
81 (0)	482 (38)	80 (0)	477 (17)
86 (1)	518 (4)	85 (1)	508 (1)
93 (1)	551 (16)	90 (0)	539 (12)
99 (1)	610 (96)	97 (1)	606 (99)
111 (0)	618 (99)	108 (0)	619 (84)
153 (4)	634 (186)	156 (1)	631 (176)
158 (11)	674 (7)	166 (13)	674 (2)
228 (8)	2002 (130)	237 (6)	1919 (6)
345 (72)	2019 (868)	336 (38)	1932 (784)
358 (2)	2057 (596)	359 (38)	1975 (430)
377 (12)	2062 (1449)	384 (15)	1981 (1130)
400 (13)	2090 (2282)	409 (24)	2008 (2213)
427 (59)	2149 (15)	440 (1)	2060 (5)
432 (1)		448 (56)	

As noted above, the high symmetry D_{3h} structure of $Cr_2(CO)_9$ is predicted to lie only ∼1 kcal/mol above the C_s structure. Candidly, it is not possible to exclude the possibility that the D_{3h} structure is the true global minimum, as DFT methods sometimes incorrectly favor lower symmetry structures. Thus the D_{3h} vibrational frequencies are of interest (Table 4). The bridging CO stretches for the D_{3h} structure are predicted (BP86)

TABLE 4: BP86 Harmonic Vibrational Frequencies (cm^{-1}) and Their Infrared Intensities (km/mol, in Parentheses) for the $Cr_2(CO)_9$ Structure, of D_{3h} Symmetry

a_1''	
41 (0)	425 (0)
a_1'	
82 (0)	667 (0)
280 (0)	1911 (0)
370 (0)	2059 (0)
472 (0)	
a_2''	
96 (1)	464 (4)
169 (18)	610 (264)
380 (341)	2004 (2462)
a_2'	
49 (0)	459 (0)
376 (0)	
e''	
87 (0)	508 (0)
87 (0)	508 (0)
113 (0)	623 (0)
113 (0)	623 (0)
270 (0)	−138 (0)
270 (0)	−138 (0)
441 (0)	1978 (0)
441 (0)	1978 (0)
e'	
56 (0)	470 (7)
56 (0)	470 (7)
86 (0)	531 (1)
86 (0)	531 (1)
92 (1)	608 (96)
92 (1)	608 (96)
365 (0)	1923 (783)
365 (0)	1923 (783)
439 (6)	1982 (1431)
439 (6)	1982 (1431)

at 1911 (a_1') and 1923 (e') cm^{-1}. The terminal CO stretches are similarly predicted at 1978 cm^{-1} (e''), 1982 cm^{-1} (e'), 2004 cm^{-1} (a_2'') and 2059 cm^{-1} (a_1'). The most intense IR fundamental is predicted at 2004 cm^{-1} (intensity 2462 km/mol). The analogy with the C_s frequencies is strong, as expected, since the D_{3h} and C_s structures are closely related.

3.3. Thermochemistry. Thermodynamically, the dissociation energy of $Cr_2(CO)_9$ to $Cr(CO)_4$ and $Cr(CO)_5$ fragments is predicted to be 32 kcal/mol with the B3LYP functional or 43 kcal/mol with the BP86 functional, while dissociation to $Cr(CO)_3$ and $Cr(CO)_6$ fragments is predicted to be 30 kcal/mol (B3LYP) or 41 kcal/mol (BP86). This demonstrates the remarkably stronger [than predicted for $Cr_2(CO)_{11}$ and $Cr_2(CO)_{10}$] interaction between the two chromium fragments. In previous work, the unstable saturated $Cr_2(CO)_{11}$ was predicted[20] to lie above the stable dissociated fragments[25,26] $Cr(CO)_5$ and $Cr(CO)_6$ in energy and to be only slightly metastable with respect to the transition state leading to this dissociation. The barely stable $Cr_2(CO)_{10}$ was found[21] to lie 56 kcal/mol (B3LYP) above the well-known[27] $Cr_2(CO)_{10}^{2-}$; the dissociation energy to two $Cr(CO)_5$ fragments or to $Cr(CO)_6$ plus $Cr(CO)_4$ was determined to be about 10 kcal/mol.

To what might we compare our predicted $Cr_2(CO)_9$ dissociation energies? Perhaps the best comparison is with $Mn_2(CO)_{10} \rightarrow 2Mn(CO)_5$. In the latter case the B3LYP dissociation energy is 24.2 kcal/mol, while that for BP86 is 31.1 kcal/mol. As with $Cr_2(CO)_9$, the BP86 dissociation energy is larger. The experimental dissociation energy for $Mn_2(CO)_{10}$ is problematic, with the most reliable result probably the solution result of Pugh and Meyer,[28] namely 37.7 ± 4.1 kcal/mol. Weitz[29] has argued that the gas phase dissociation energy of such a system should be greater than the solution value. In any case, our comparisons seem to show unambiguously that the dissociation energy of $Cr_2(CO)_9$ is greater than that for the known molecule $Mn_2(CO)_{10}$. This supports our contention that it should be possible to make $Cr_2(CO)_9$.

In the next section, we explore the strong interaction of the fragments in $Cr_2(CO)_9$ which is so different from that in $Cr_2(CO)_{10}$ and $Cr_2(CO)_{11}$. The answer lies in analysis of the metal−metal bonding.

3.4. Metal−Metal Bonding. In terms of formal electron counting in $Cr_2(CO)_9$, each bridging CO ligand provides one electron to each metal atom. Without assuming any Cr−Cr bonding, each chromium atom with three bridging carbonyls and three terminally bonded carbonyls has 15 electrons. The 18-electron[30] rule then suggests that a direct Cr≡Cr triple bond is present. In terms of hybrid orbitals, each chromium center may be considered to be sp^3d^2 hybridized consistent with its octahedral environment. Six hybrid orbitals are used for bonding to the CO ligands, leaving the metal d_{xy}, d_{xz}, and d_{yz} orbitals for metal−metal bond formation. However, the orientations of the carbonyl ligands mean that these three orbitals available for Cr−Cr bond[31] formation do not point directly toward each other. Compared to the classic $[Re_2Cl_8]^{2-}$ molecule, the result should be a "bent" Cr−Cr bond.

Owing to the ineffective nature of d-orbital overlap as compared to s- or p-orbital overlaps, the electrons in d orbitals are more localized than those in s or p orbitals. The metal−metal bonding using d orbitals was analyzed by searching for the participation percentage of the d orbitals in each of the relevant molecular orbitals (MOs).

The MOs to which the d orbitals give the largest contributions for $Cr_2(CO)_9$ in C_s symmetry are listed in Table 2. Seven orbitals are listed from the sixth lowest occupied orbital (HOMO−5) to the first lowest unoccupied orbital (LUMO). The molecular orbital coefficient analysis shows that the main covalent contribution is directly provided by the mixing of the different percentages of d orbitals on the two chromium atoms. For instance, the HOMO−5 consists of the mixture of about 56% or 58% of the $d_{x^2-y^2}$ orbitals and about 27% or 37% of the d_{z^2} orbitals, depending upon the computational method used. The HOMO−4 is also composed of a $d_{x^2-y^2}$, d_{xy}, and d_{z^2} combination (owing to the C_s symmetry the d orbitals are inseparable).

The symmetry-adapted linear combinations of the d orbitals are graphically displayed in Figure 4 according to the chosen Cartesian coordinates, the phase of the atomic orbital, and the relative ratio of the participation percentage of the d orbital. (Note that the metal−metal bond here lies on the *y* axis.) Figures 5 and 6 show density plots of the orbitals. The results suggest that HOMO−5, HOMO−4 and HOMO−3 are the bonding orbitals among the six highest occupied orbitals. The metal orbitals with π bonding character are d_{xy}, or d_{yz}. The δ bonding orbital is d_{xz}, and the distorted σ bonding orbitals are $d_{x^2-y^2}$ and d_{z^2} (owing to the distortion of the pair of CrC_6 octahedra). The corresponding antibonding orbitals are HOMO−2 to HOMO. Notably, there is a substantial energy gap (−6.41 to −7.08 eV) between the lowest antibonding orbital HOMO−2 and the highest bonding orbital HOMO−3, which confirms the existence of the overlaps between the d_{yz} orbitals and the d_{xz} orbitals in HOMO−3. The main contribution to the metal−metal bond comes from the d_{yz} orbitals in a π bond after considering the smaller overlap of the d_{xz} orbitals to form a δ bond. The HOMO−4 and HOMO−5 are stabilized by the bonding of the d_{xy}, $d_{x^2-y^2}$, and d_{z^2} orbitals. In the HOMO−4, the stabilization

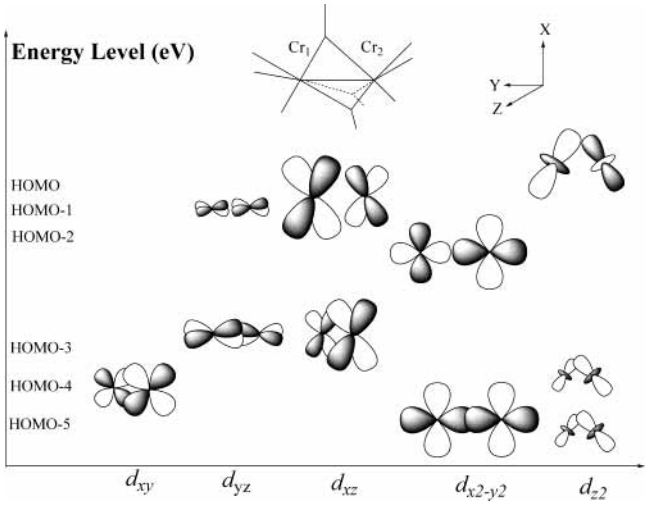

Figure 4. Symmetry-adapted linear combinations of the d atomic orbitals of the metal atoms (Cr_1 and Cr_2 assigned in Figure 3) for the molecular energy levels of the singlet $Cr_2(CO)_9$ with C_s symmetry.

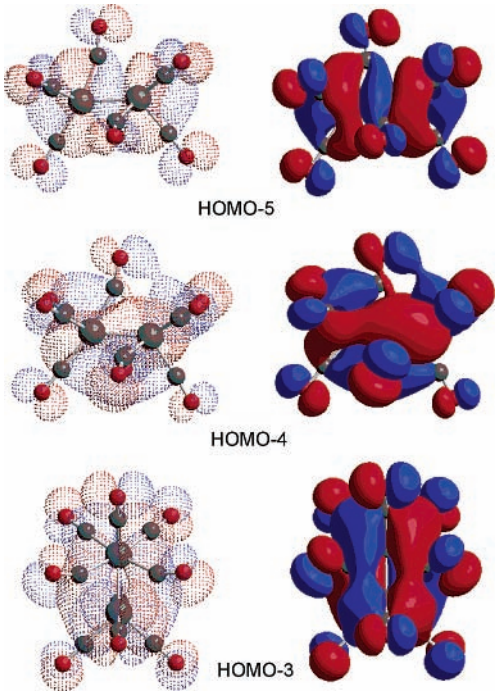

Figure 5. Molecular orbital plots of bonding orbitals of singlet $Cr_2(CO)_9$ in C_s symmetry, showing from the sixth valence molecular orbital HOMO−5 from the HOMO up to HOMO−3. For HOMO−5, the C_s plane is in the plane of the paper (*xy* plane) and viewed along the *z* axis. For HOMO−4, shown similarly to the HOMO−5. For HOMO−3, the C_s plane is perpendicular to the plane of the paper (*xz* plane) and viewed along the *x* axis.

of this energy level arises from the bonding of the d_{xy} and d_{z^2} orbitals if the small contribution from the $d_{x^2-y^2}$ is neglected. The presence of the bonding of the d_{xy} and d_{z^2} orbitals makes HOMO−4 lower than HOMO−3 by 7.21 − 7.08 = 0.13 eV. The HOMO−5 is lowered mainly by the $d_{x^2-y^2}$ bonding orbitals from 7.43 to 7.21 eV. Thus we obtain the three d−d bonding MOs for the metal−metal bond.

Interestingly, the two antibonding orbitals (HOMO−1 and HOMO−2) are almost degenerate in energy, which may be consistent with the two symmetrical bridging carbonyls with respect to the C_s plane. The HOMO itself is slightly higher in energy than the degenerate occupied antibonding MOs. HOMO−1 and HOMO−3 are a pair of bonding and antibonding orbitals

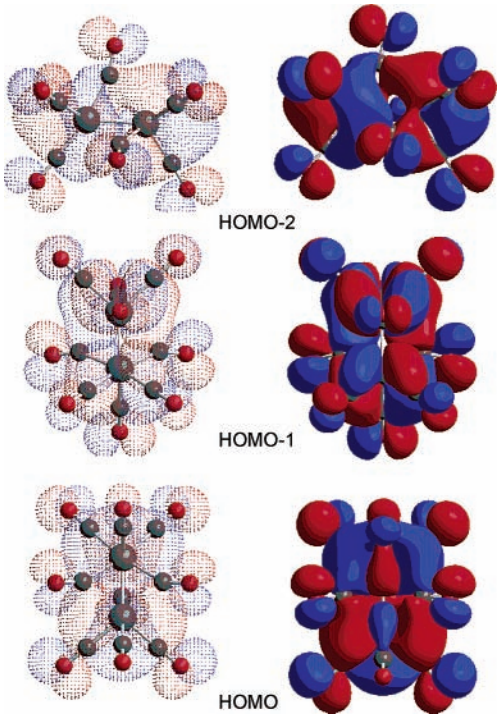

Figure 6. Molecular orbital plots of antibonding orbitals of singlet $Cr_2(CO)_9$ in C_s symmetry, showing from the third valence molecular orbital HOMO−2 from the HOMO up to the HOMO. For HOMO−2, the C_s plane is in the plane of the paper (*xy* plane) and viewed along the *z* axis. For HOMO−1, the C_s plane is perpendicular to the paper plane (*xz* plane) and viewed from the *x* axis. For HOMO, shown similarly to the HOMO−1.

with δ character. The relatively larger energy gap between the three bonding orbitals suggests that more electron density accumulates in the bonding orbitals between the two metals. In other words, the d_{xy}, d_{yz}, and d_{xz} orbitals contribute to the stabilization of this compound. Thus the metal−metal bond is mainly composed of two degenerate π bonds and one δ bond.

Also significant is the large gap between the HOMO and LUMO which measures the chromium−chromium bond stability in $Cr_2(CO)_9$. The large energy difference indicates the singlet configuration is the favored state rather than the triplet. At the same time it shows the singlet configuration is the dominant configuration among all the correlated configurations.

In practice, molecular orbitals involve combinations of all available atomic orbitals. In addition to the d orbitals of the metal atoms, s and p orbitals from the carbonyl groups also make contributions to the MOs. Thus Cr−CO σ and π bonding have a major effect on the shapes and energies of the MOs as well as the chromium−chromium bonding discussed above. Nevertheless, the MO plots provide useful insight into the nature of the chromium−chromium multiple bond in $Cr_2(CO)_9$ and suggest that $Cr_2(CO)_9$ is a potentially stable molecule in contrast to $Cr_2(CO)_{10}$ and $Cr_2(CO)_{11}$.

4. Discussion

We emphasize that these interactions occur in the framework of the complex; without the ligands such bonding could not be reasonably described by DFT. Distinction must be made between genuine transition metal *complexes*, cases in which ligands are attached to chromium, and the bare chromium−chromium dimer, where virtually all methods fail. Massive multiconfigurational character occurs in the latter, where the only interaction occurring is that of a chromium atom with another chromium. Studies at various levels of theory, including CCSD,[32]

CCSD(T),[33] various DFT,[34−36] CASPT2,[37,38] CASPT2 with relativistic corrections,[39] MRACPF plus relativistic corrections,[40] and CASSCF plus an Epstein−Nesbet second-order perturbation treatment,[41] found a wide range of bond lengths and frequencies. The chromium dimer remains a difficult case for the most sophisticated methods. Even the recent study by Dachsel, Harrison, and Dixon[42] employing a very large MRCI/MRACPF was not in entirely adequate agreement with experiment. The CASPT2 method appears to be the most successful to date, and an excellent review has recently been given by Roos.[43] These theoretical challenges result from the inability of most methods to describe the bonding situation: formally, the chromium−chromium dimer has a bond order of six but with a low dissociation energy (<2 eV). This phenomenon, however, is an uncommon circumstance, as noted by Siegbahn and Blomberg in their recent review of DFT applied to transition metal systems:[44] "The (extreme) multiple bonding is almost unique with its severe near-degeneracy problems, so this situation does not need to be accurately described by a method used to study more normal chemical systems." They note that this recognition that metal behavior is different in complexes has paved the way for diverse applications of DFT to transition metal complexes: "Another significant insight gained from the modeling of transition-metal complexes is that some of the problems encountered early, which were thought to be necessary to solve, are in fact very atypical for transition-metal complexes. The examples of the nickel atom and the chromium dimer ... are illustrative of this point."

Regarding this point, Morokuma[45] also noted, "The established problem of the s^0 d^n vs s^1d^{n-1} description by DFT methods dominates the picture for coordinatively unsaturated molecules, but should not play any role for systems [with more ligands]." Several such studies with DFT confirm this finding.[46−48]

We could ask the question of at what point will the homoleptic carbonyl dimetallic system fail to be described by DFT? To this end, we compare $Cr_2(CO)_9$ to less unsaturated structures. The optimized structure for $Cr_2(CO)_9$ (**I**), like those for singlet $Cr_2(CO)_{10}$ (**II**) and $Cr_2(CO)_{11}$ (**III**), retains an approximately octahedral environment of the six carbonyl groups around each chromium atom similar to that in the very stable $Cr(CO)_6$. Thus the structures of $Cr_2(CO)_{11}$ (**III**), $Cr_2(CO)_{10}$ (**II**), and $Cr_2(CO)_9$ (**I**) may be regarded as consisting of two $Cr(CO)_6$ octahedra with a vertex, edge, and face in common, respectively. However, the structure of $Cr_2(CO)_9$ (**I**) is unique among the three structures **I**, **II**, and **III** in having the two chromium atoms close enough together for strong metal−metal bonding. Furthermore, the metal−metal distance of 2.31 Å (B3LYP) or 2.28 Å (BP86) is consistent with the Cr≡Cr triple bond required to give each chromium atom the favored 18-electron rare gas electronic configuration as indicated by the experimentally determined Cr≡Cr distance of 2.28 Å in (η^5-$Me_5C_5)_2Cr_2(CO)_4$ (**IV**),[49] also required to be a triple bond in order to give each chromium atom the favored 18-electron rare gas electronic configuration. The metal−metal bond analysis in $Cr_2(CO)_9$ (**I**) indicates that the main covalent contribution is provided by the d orbitals of the chromium atoms, not by the p orbitals of the bridging carbonyls. The metal−metal triple bond thus was found to consist of two π bonds, together with a weak δ bond. This Cr≡Cr triple bond thus differs significantly from the familiar carbon−carbon triple bond in acetylene, which consists of two π bonds and a σ bond.

One should note that our affinity for some sort of bond order−bond distance relationship is not universally held. A minority, but still substantial view, is that bond order−bond distance

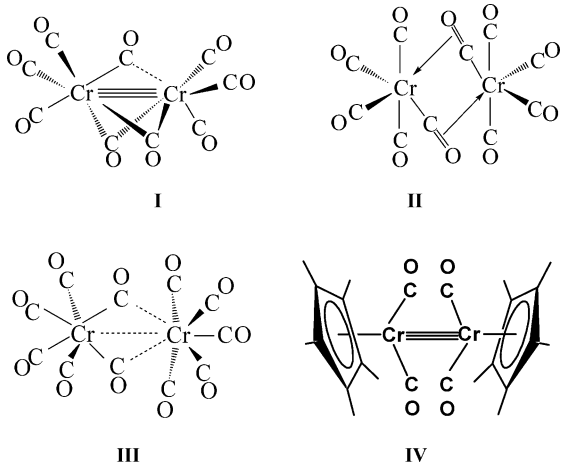

I **II**

III **IV**

correlations are meaningless, and that bond order can only be determined via electron density analysis. Without criticizing this approach, we are more comfortable with relating bond orders to quantities more familiar to experimentalists, e.g., bond distances, rotational barriers, and force constants.

Overall $Cr_2(CO)_9$ (**I**) is a thermodynamically stable compound and should be isolable experimentally. However, a feasible synthetic route would need to avoid $Cr_2(CO)_{11}$ or $Cr_2(CO)_{10}$ intermediates, since these have been shown in our previous papers[11,12] to be thermodynamically unstable with respect to mononuclear species. A possible method to synthesize $Cr_2(CO)_9$ (**I**) might be to combine $Cr(CO)_5$ and $Cr(CO)_4$ fragments generated by decomposition of labile octahedral $L_2Cr(CO)_4$ and $LCr(CO)_5$ derivatives. In this connection, the binuclear manganese derivative (η^5-$Me_5C_5)_2Mn_2(\mu$-$CO)_3$ (**V**)

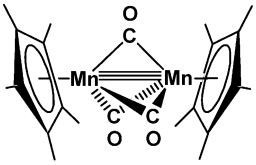

V

has been isolated by the spontaneous decomposition of (η^5-Me_5C_5)Mn$(CO)_2$THF.[50] This manganese compound (**V**) is closely related to the optimized structure for $Cr_2(CO)_9$ (**I**) by substitution of each $Cr(CO)_3$ unit linked by the three bridging carbonyls with an isoelectronic and isolobal (η^5-Me_5C_5)Mn unit. Thus (η^5-$Me_5C_5)_2Mn_2(\mu$-$CO)_3$ (**V**) would be expected to have an Mn≡Mn triple bond similar to the Cr≡Cr triple bond found for $Cr_2(CO)_9$ (**I**). In this connection determination of the structure of (η^5-$Me_5C_5)_2Mn_2(\mu$-$CO)_3$ (**V**) by X-ray diffraction indicates an Mn≡Mn distance of 2.17 Å.[51] This short distance is consistent with a metal−metal triple bond similar to that suggested for $Cr_2(CO)_9$ (**I**) after making allowance for differences in the electronic properties of carbonyl and pentamethylcyclopentadienyl ligands.

5. Conclusion and Outlook

In this research a stable $Cr_2(CO)_9$ molecule is predicted with a chromium−chromium bond having a relatively short metal−metal distance of about 2.3 Å. Based on the comparison to other well-known metal carbonyl compounds, our calculated distances appear reasonable. The Cr−Cr distance is similar to that of the triply bonded (pentamethyl Cp)$_2Cr_2(CO)_4$ compound[44] but significantly longer than 1.96 Å in a quadruply bonded dichromium tetracarboxylate[52] with its $\sigma^2\pi^4\delta^2$ configuration.[53]

Thus the theoretical distance is reasonable as the σ component (which is expected to be the major contributor to the length of the Cr−Cr bond) is missing in $Cr_2(CO)_9$. Such theoretical insights give this work the potential to serve as inspiration for synthetic chemists to go to the bench and try to prepare $Cr_2(CO)_9$, predicted to be a makeable molecule.

Though DFT predicts $Cr_2(CO)_9$ to be a stable compound with a rather labile structure and a unique sort of metal−metal bond, we anticipate a point at which DFT will not be useful for some $Cr_2(CO)_x$ ($x < 8$). Certainly, the bare metal dimer is not describable with DFT. We would hope the work of this paper would be a step along the pathway to discovering the point at which there are no longer enough ligands for a $Cr_2(CO)_x$ species to behave as a "normal" molecule. Such work would give further insight into both DFT methods in general and the infamous bare chromium dimer problem in particular as well as provide novel insights into even more highly saturated homoleptic dimetallic chromium compounds.

Acknowledgment. We are grateful for the support of this work by NSF Grant CHE-0136186. We thank Dr. Yukio Yamaguchi for helpful discussions about the metal−metal bonding, Dr. Wang Zhi Xiang for guidance in the analysis of the electron density, and Dr. Steven S. Wesolowski for help in producing the orbital plots as well as several helpful discussions. We also thank the referees for their helpful suggestions and insights.

Note Added after ASAP Posting. This article was posted ASAP on 10/29/03. Two data values were corrected in the 3.3. Thermochemistry section. The article was reposted 11/14/03.

References and Notes

(1) Shyu, S.-G.; Calligaris, M.; Nardin, G.; Wojcicki, A. *J. Am. Chem. Soc.* **1987**, *109*, 3617.
(2) Wong, W.-T.; Wong, W.-K. *Acta Crystallogr., Sect. C* **1994**, *C50*, 1404.
(3) Maitra, K.; Catalano, V. J.; Nelson, J. H. *J. Organomet. Chem.* **1997**, *529*, 409.
(4) Adams, R. D.; Kwon, O.; Smith, M. D. *J. Organomet. Chem.* **2002**, *41*, 6281.
(5) Garcia, M. E.; Riera, V.; Ruiz, M. A.; Saez, D.; Vaissermann, J.; Jeffery, J. C. *J. Am. Chem. Soc.* **2002**, *124*, 14304.
(6) Chisholm, M. H.; Davidson, E. R.; Quinlan, K. B. *J. Am. Chem. Soc.* **2002**, *124*, 15351.
(7) Macchi, P.; Garlaschelli, L.; Sironi, A. *J. Am. Chem. Soc.* **2002**, *124*, 14173.
(8) Hall, M. B. In *Electron Distribution and the Chemical Bond*; Coppens, P., Hall, M. B., Eds.; Plenum Press: New York, 1982; p 205.
(9) Xie, Y.; Schaefer, H. F.; King, R. B. *J. Am. Chem. Soc.* **2000**, *122*, 8746.
(10) Winter, M. J. *Adv. Organomet. Chem.* **1989**, *29*, 101.
(11) Richardson, N. A.; Xie, Y.; King, R. B.; Schaefer, H. F. *J. Phys. Chem. A* **2001**, *105*, 11134.
(12) Li, S.; Richardson, N. A.; Xie, Y.; King, R. B.; Schaefer, H. F. *Faraday Discuss.* **2003**, *124*, 315.
(13) Jezowska-Trzebiatowska, B.; Nissen-Sobocinska, B. *J. Organomet. Chem.* **1987**, *322*, 331.
(14) Dunning, T. H. *J. Chem. Phys.* **1970**, *53*, 2823.
(15) Huzinaga, S. *J. Chem. Phys.* **1965**, *42*, 1293.
(16) Wachters, A. J. H. *J. Chem. Phys.* **1970**, *52*, 1033.
(17) Hood, D. M.; Pitzer, R. M.; Schaefer, H. F. *J. Chem. Phys.* **1979**, *71*, 705.
(18) Ziegler, T. *Can. J. Chem.* **1995**, *73*, 743.
(19) Becke, A. D. *J. Chem. Phys.* **1993**, *98*, 5648.
(20) Lee, C.; Yang, W.; Parr, R. G. *Phys. Rev. B* **1988**, *37*, 785.
(21) Jonas, V.; Thiel, W. *Organometallics* **1998**, *17*, 353.
(22) Becke, A. D. *Phys. Rev. A* **1988**, *38*, 3098.
(23) Perdew, J. P. *Phys. Rev. B* **1986**, *33*, 8822; *Phys. Rev. B* **1986**, *34*, 7046.
(24) Frisch, M. J.; Trucks, G. W.; Schlegel, H. B.; Gill, P. M. W.; Johnson, B. G.; Robb, M. A.; Cheeseman, J. R.; Keith, T. A.; Petersson, G. A.; Montgomery, J. A.; Raghavachari, K.; Al-Laham, M. A.; Zakrzewski, V. G.; Ortiz, J. V.; Foresman, J. B.; Cioslowski, J.; Stefanov, B. B.; Nanayakkara, A.; Challacombe, M.; Peng, C. Y.; Ayala, P. Y.; Chen, W.; Wong, M. W.; Andres, J. L.; Replogle, E. S.; Gomperts, R.; Martin, R. L.; Fox, D. J.; Binkley, J. S.; Defrees, J. D.; Baker, J.; Stewart, J. P.; Head-Gordon, M.; Gonzalez, C.; Pople, J. A. *Gaussian 94*, revision B.3; Gaussian, Inc.: Pittsburgh, PA, 1995.
(25) Barnes, L. A.; Liu, B.; Lindh, R. *J. Chem. Phys.* **1993**, *98*, 3978.
(26) Rees, B.; Mitschler, A. *J. Am. Chem. Soc.* **1976**, *98*, 7918.
(27) Borrmann, H.; Pirani, A. M.; Schrobilgen, G. J. *Acta Crystallogr., Sect. C* **1997**, *53*, 19.
(28) Pugh, J. R.; Meyer, T. J. *J. Am. Chem. Soc.* **1992**, *114*, 3784.
(29) Weitz, E. J. *J. Phys. Chem.* **1994**, *98*, 11256.
(30) Green, M. L. H. *J. Organomet. Chem.* **1995**, *500*, 127.
(31) Cotton, F. A.; Wilkinson, G.; Murillo, C. A.; Bochmann, M. *Advanced Inorganic Chemistry*, 6th ed.; Wiley and Sons: New York, 1999. Cotton, F. A.; Walton, R. A. *Multiple Bonds Between Metal Atoms*; Clarendon Press: Oxford, 1993.
(32) Scuseria, G. E. *J. Chem. Phys.* **1991**, *94*, 442.
(33) Scuseria, G. E.; Schaefer, H. F. *Chem. Phys. Lett.* **1990**, *174*, 501.
(34) Bauschlicher, C. W.; Partridge, H. *Chem. Phys. Lett.* **1994**, *231*, 277.
(35) Barden, C. A.; Rienstra-Kiracofe, J. C.; Schaefer, H. F. *J. Chem. Phys.* **2000**, *113*, 690.
(36) Yanagisawa, S.; Tsuneda, T.; Hirao, K. *J. Chem. Phys.* **2000**, *112*, 545.
(37) Andersson, K. *J. Chem. Phys.* **1995**, *237*, 212.
(38) Mitrushenkov, A. O.; Palmieri, P. *Chem. Phys. Lett.* **1997**, *278*, 285.
(39) Andersson, K.; Roos, B. O.; Malmqvist, P. A. *Chem. Phys. Lett.* **1999**, *103*, 152.
(40) Stoll, H.; Werner, H. J. *Mol. Phys.* **1996**, *88*, 793.
(41) Roos, B. O.; Andersson, K. *Chem. Phys. Lett.* **1995**, *245*, 215.
(42) Dachel, H.; Harrison, R. J.; Dixon, D. A. *J. Phys. Chem. A* **1999**, *103*, 152.
(43) Roos, B. O. *Collect. Czech Chem. Commun.* **2003**, *68*, 265.
(44) Siegbahn, P. E. M.; Blomberg, M. R. A. *Chem. Rev.* **2000**, *100*, 421.
(45) Khoroshun, D. V.; Djamaladdin, G. M.; Vreven, T.; Morokuma, K. *Organometallics* **2001**, *20*, 2007.
(46) Koch, W.; Holthausen, M. C. *A Chemist's Guide to Density Functional Theory*; Wiley-VCH: Weinheim, FRG, 2000; pp 251−259.
(47) Holthausen, M. C.; Fiedler, A.; Schwarz, H.; Koch, W. *J. Phys. Chem.* **1996**, *100*, 6236.
(48) Holthausen, M. C.; Koch, W. *J. Am. Chem. Soc.* **1996**, *118*, 9932.
(49) Potenza, J.; Giordano, P.; Mastropaolo, D.; Efraty, A. *Inorg. Chem.* **1974**, *13*, 2540.
(50) Herrmann, W. A.; Serrano, R.; Weichmann, J. *J. Organomet. Chem.* **1983**, *246*, C57.
(51) Bernal, I.; Korp, J. D.; Hermann, W. A.; Serrano, R. *Chem. Ber.* **1984**, *117*, 434.
(52) Cotton, F. A.; Hillard, E. A.; Murillo, C. A.; Zhou, H. *J. Am. Chem. Soc.* **2000**, *122*, 416. For a more general discussion of Cr−Cr quadruple bonds, see: Ketkar, S. N.; Fink, M. *J. Am. Chem. Soc.* **1985**, *107*, 338.
(53) Note that in going from $Cr_2(CO)_9$ to $Cr_2(CO)_8$ the number of formal metal−metal bonding electrons increases from six to eight. This is because removal of a bridging CO from $Cr_2(CO)_9$ returns one electron, in a simple picture, to each chromium atom.